N2 in deep subsurface fracture fluids of the Canadian Shield: Source and possible recycling processes

Long Li, Kan Li, Thomas Giunta, Oliver Warr, Jabrane Labidi, Barbara Sherwood Lollar

N_2 in deep subsurface fracture fluids of the Canadian Shield: Source and possible recycling processes

Long Li[1,2*], Kan Li[1], Thomas Giunta[2,3], Oliver Warr[2], Jabrane Labidi[4], Barbara Sherwood Lollar[2]

1. Department of Earth and Atmospheric Sciences, University of Alberta, Edmonton, Alberta, Canada
2. Department of Earth Sciences, University of Toronto, Toronto, Ontario, Canada
3. IFREMER, Unité des Géosciences Marines, 29280 Plouzané, France
4. Université de Paris, Institut de Physique du Globe de Paris, Université Paris Diderot, 75005 Paris, France

* Corresponding author (email: long4@ualbertaca)

Key Words

Nitrogen cycle, Canadian Shield, deep subsurface, abiotic nitrogen reduction, microbial ammonium oxidation

Abstract: In addition to high concentrations of CH_4 and H_2, abundant dissolved N_2 is found in subsurface fracture fluids in Precambrian cratons around the world. These fracture fluids have hydrogeological isolation times on order of thousands to millions and even billions of years. Assessing the sources and sinks of N_2 and related (bio)geochemical processes that drive the nitrogen cycle in these long isolated systems can shed insights into the nitrogen cycles on early Earth with implications for other planets and moons. In this study, we collected dissolved gas samples from deep subsurface fracture fluids at seven sites (Kidd Creek, LaRonde, Nickel Rim, Fraser, Copper Cliff South, Thompson, and Birchtree) in the Canadian Shield. Multiple gas components (e.g., H_2, O_2 and Ar) were integrated with $\delta^{15}N_{N2}$ values to characterize the N_2 signatures. Results show that the dissolved N_2 in deep subsurface fracture fluids from the Canadian Shield sites are more ^{15}N-enriched than those from the Fennoscandian Shield and the Witwatersrand Basin in the Kaapvaal Craton. The nitrogen isotopic signatures of the Canadian Shield samples coupled with their hydrogeological framework indicate the N_2 was sourced from fixed ammonium in silicate minerals in host rocks and was generated by metamorphic devolatilization. Modeling of nitrogen devolatilization from host rocks supports this interpretation, but also suggests that a second process, likely abiotic N_2 reduction, is required to account for the observed ^{15}N enrichment in the N_2 samples from the Canadian Shield. A 10-year monitoring study for one of the boreholes, at 2.4 km of the Kidd Creek Observatory, shows a steady decrease in $\delta^{15}N_{N2}$ values with time, which coincides with the temporal isotopic evolution of some other gas components in this borehole. Although it cannot be confirmed at this time, this isotopic shift in N_2 may be potentially attributed to microbial processes (e.g., anaerobic oxidation of ammonium). Nevertheless, the large ^{15}N enrichments for the majority of the samples in this study suggest that the nitrogen cycle in the deep saline fracture fluids in the Canadian Shield is dominated by abiotic processes. This is in contrast to the nitrogen cycles in the subsurface fracture fluids in the Fennoscandian Shield and the Witwatersrand Basin, which have been shown to be strongly affected by extant microbial ecosystems discovered in those fracture waters.

1. Introduction

Precambrian cratons occupy the majority of the Earth's continental crust (> 70% by surface area; Goodwin, 1996). These remnants of early Earth's crust are dominated by (meta-)igneous rocks varying from ultramafic to felsic in composition (e.g., Hoffmann, 1989). Abundant fractures developed over the history of these igneous rocks host a large terrestrial subsurface water reservoir of up to 30% of the planet's total groundwater inventory (Warr et al., 2018). Geochemical signatures (e.g., salinity, major and trace elemental compositions, dissolved gas contents, redox condition, $\delta^{18}O$ and $\delta^{2}H$) of these fluids indicate that they have been strongly influenced by water-rock reactions, and, in some cases, affected by mixing with varying amounts of secondary (paleo-)meteoric water (e.g., Ward et al., 2004; Onstott et al., 2006; Li et al., 2016; Heard et al., 2018; Warr et al., 2021a and references therein). Most of these deep subsurface fracture water systems have been hydrogeologically isolated over geological time scales, e.g., up to hundreds of million years to billions of years in the Canadian Shield (Holland et al., 2013; Warr et al., 2018), up to tens to hundreds of million years in the Fennoscandian Shield (Kietäväinen et al., 2014) and the Witwatersrand Basin in the Kaapvaal Craton, South Africa (Heard et al., 2018; Lippmann et al., 2003). Closed-system water-rock interactions over these extended time periods has progressively produced chemicals (e.g., H_2, hydrocarbons, sulfate) and highly reducing habitable environments favorable for chemo(litho)trophic microbes (Lin et al., 2005, 2006; Li et al., 2016; Magnabosco et al., 2018; Lollar et al., 2019).

Studies of the subsurface fracture fluids from the Kaapvaal Craton, the Canadian Shield and the Fennoscandian Shield have identified some general quasi-depth-controlled variations in geochemistry and microbial community attributed to the degree of penetration of (paleo-)meteoric water into the subsurface (Warr et al;., 2021a and references therein). Based on

noble gas studies, the shallower fracture fluids generally have shorter residence times, whereas the deeper, more saline fracture fluids have longer residence times (Lippmann et al., 2003; Lippmann-Pipke et al., 2011; Heard et al., 2018; Warr et al., 2018; 2021a). The shallow fracture fluids are mostly highly oxidizing fresh to brackish waters, and contain abundant biomass with diverse microbial communities; in contrast, the deep fracture fluids are mostly highly reducing saline to brine waters, and contain low-abundance biomass with less microbial diversity (e.g., Ward et al., 2004; Onstott et al., 2006; Lin et al., 2006; Magnabosco et al., 2015; Lollar et al., 2019).

These geochemical and microbiological differences can directly impact the isotopic signatures of the dissolved gaseous components in the fracture fluids. For example, different carbon recycling pathways have been clearly identified in these fracture fluids based on the carbon and hydrogen isotopic signatures of CH_4 and other light n-alkanes (e.g., Sherwood Lollar et al., 1993a, b, 2002, 2006, 2008; Ward et al., 2004; Warr et al., 2021b) and clumped isotopic signatures of CH_4 and N_2 (Young et al., 2017; Labidi et al., 2020; Warr et al., 2021b). These studies have reported consistent observations from both the Canadian Shield and the Kaapvaal Craton suggesting that CH_4 in the shallower fracture fluids is dominantly microbial, whereas CH_4 in the deeper, more saline fracture fluids with longer residence times can show predominantly abiogenic signatures (Sherwood Lollar et al., 2006; 2008, 2021; Warr et al., 2021b;). More recently, formate and acetate in fluids at 2.4 to 3 km below surface (kmbs) at one of the key deep subsurface sites of the Canadian Shield, the Kidd Creek (KC) Observatory, have been demonstrated to be produced by abiotic organic synthesis (Sherwood Lollar et al., 2021). Multiple sulfur isotopic signatures of dissolved sulfate in fluids from 2.4 kmbs of the KC

88 Observatory also indicate that the dissolved sulfate in these fluids was derived from abiotic
89 process by indirect radiolytic oxidation of sulfide minerals in host rocks (Li et al., 2016).
90 Despite numerous studies on the carbon and sulfur cycles in the subsurface fracture fluids
91 in Precambrian cratons, to date, the cycle of another life-constituting element, nitrogen, has not
92 been well examined, particularly in the Canadian Shield. N_2 is typically the second largest
93 dissolved gas component by volume in subsurface fracture fluids in Precambrian cratons around
94 the world. In an earlier study, Sherwood Lollar et al. (1993a) reported the $\delta^{15}N$ values of N_2
95 collected from fracture fluids in the Fennoscandian Shield and the Canadian Shield. Thirteen N_2
96 samples from the Fennoscandian Shield show a $\delta^{15}N$ range from 0.2‰ to 5.1‰ (with one high
97 value of 10.0‰), whereas four N_2 samples from the Canadian Shield mostly show higher $\delta^{15}N$
98 values (Thompson: 1.4‰; Matagami: 8.6‰; Norita: 11.8‰; Val d'Or: 9.1‰). Labidi et al.
99 (2020) also reported two $\delta^{15}N$ data from Sudbury (2.6‰ and 2.8‰) and two $\delta^{15}N$ data from the
100 KC Observatory (6.6‰ and 6.8‰). Dissolved N_2 in subsurface fracture fluids from the
101 Witwatersrand Basin in the Kaapvaal Craton was studied by Silver et al. (2012). After correction
102 for air contamination using the N_2/O_2 ratio as an index, a $\delta^{15}N_{N2}$ range from –1.3‰ to 5.8‰ was
103 yielded and considered to result from complicated geochemical and, more importantly,
104 biological recycling processes (Silver et al., 2012).
105 The relatively few $\delta^{15}N$ data from the Canadian Shield make it difficult to compare with
106 those from the Fennoscandian Shield and the Kaapvaal Craton for the understanding of nitrogen
107 cycle in subsurface fracture fluids in Precambrian cratons. In this context, it is important to carry
108 out a more comprehensive investigation of N_2 in deep fracture fluids in the Canadian Shield,
109 particularly those from the KC Observatory. The KC Observatory located in Timmins (Ontario)
110 is an iconic site for the study of subsurface fracture fluids, given the tremendous knowledge

about this site accumulated from studies over nearly three decades (e.g., Sherwood Lollar et al., 1993a, b, 2002, 2021; Doig et al. 1995; Holland et al., 2013; Li et al., 2016; Lollar et al., 2019). In particular, long-term monitoring has been possible at an observatory location 2.4 kmbs since 2007, commencing shortly after the exploratory boreholes were drilled. Noble gas studies indicate that the mean residence times of the fluids at KC were extremely long (e.g., 1.0 – 2.2 Ga at 2.9 kmbs; Warr et al., 2018), while hydrogeological draining of the fluids may result in some boreholes decreasing in age over time (e.g., at 2.4 kmbs, initially 1.1 – 1.7 Ga but has decreased to 0.2 – 0.6 Ga recently; Holland et al., 2013, Warr et al., 2018). To date, these fluids show the presence of chemolithotrophic organisms (sulfate-reducing organisms in particular) but with low biomass and low rates of activity (Li et al., 2016; Lollar et al., 2019; Sherwood Lollar et al., 2021; Warr et al., 2021b). The geochemical and isotopic signatures of these fluids (including dissolved components) may represent the closest abiotic end-members available in the terrestrial deep subsurface (e.g., Sherwood Lollar et al., 2021; Warr et al., 2021b). Such abiotically dominated sites provide a valuable opportunity to assess the long-term abiotic nitrogen recycling processes occurring in these highly reducing waters. This knowledge may further provide crucial insights into the geochemical processes that could have influenced the origin and early evolution of life on the early Earth, and inform models of possible habitability on other planets and moons (NASEM, 2019).

Here we report the gas concentrations and $\delta^{15}N_{N2}$ values of 45 samples from 7 sites in the Canadian Shield (Fig. 1). In particular, 25 samples were collected from the KC Observatory from 2.1 to 2.9 kmbs, and at the 2.4 kmbs sampling location, over a temporal span of 10 years (2007-2017). This sample suite provides a high-density dataset to evaluate the spatial and temporal changes of the nitrogen cycle in these fracture water systems. Aiming to better constrain the

nitrogen source and recycling processes in the fracture fluids in the Canadian Shield, bulk-rock nitrogen concentrations and isotope compositions were also analyzed on 23 host rock samples from KC, Sudbury, and Thompson. For comparison, nitrogen isotope compositions were also measured on refractory carbon component in 6 graphite-bearing samples from KC.

2. Geological background and samples

The samples in this study were collected from two sites in the Abitibi greenstone belt (i.e., KC and LaRonde), three sites in the Sudbury Basin (i.e., Copper Cliff South, Nickel Rim, and Fraser), and two neighboring sites (Birchtree and Thompson) in the Thompson nickel belt in the western Superior boundary zone, near Thompson, Manitoba (Fig. 1).

The KC Observatory in Ontario is geologically located in the volcanic successions of the Kidd-Munro assemblage in the Abitibi. The host rocks at KC include 2.71 – 2.72 Ga ultramafic, mafic (gabbros and basalts) to felsic (mainly rhyolites) rocks with graphite-bearing lenses formed in a rifting sub-proximal seafloor setting (Bleeker and Parrish, 1996; Hannington et al., 1999; Prior et al., 1999). The rocks experienced regional metamorphism which started at 2.69 Ga, reached peak metamorphism of greenschist facies (~ 400 ºC) at 2.64 Ga, and ended as late as 2.60 Ga locally (Barrie and Davis, 1990; Smith et al., 1993; Davis et al., 1994; Bleeker et al., 1999; Powell et al., 2011).

LaRonde (LR) in Quebec is geologically located in the Bousquet formation of the 2.7 Ga Blake River group in the Abitibi. The host rocks are composed of a continuous magmatic series of tholeiitic – transitional mafic to felsic rocks in the lower member, and transitional – calc-alkaline intermediate to felsic rock in the upper member (Mercier-Langevin et al., 2007). The

156 rocks experienced a prograde metamorphism to upper greenschist – lower amphibolite facies and
157 a subsequent greenschist-facies retrograde metamorphism (Dimroth et al., 1983).

158 Copper Cliff South (CCS), Nickel Rim (NR) and Fraser (FR) are all in the Sudbury
159 impact basin (Ontario). The dominant rock assemblage in the region is the Sudbury Impact
160 Complex (SIC) which was formed by meteoritic impact-induced melting of the Archean
161 basement (Faggart et al., 1985) in ~1.85 Ga (Krogh et al., 1982; Davis, 2008). FR is in the
162 middle of the North Range and NR is in the east of the South Range of the SIC. Both sites
163 geologically lie in the footwall of the SIC that is dominated by 2.64 Ga granitic rocks (Meldrum
164 et al., 1997) and Archean meta-volcanic and metasedimentary rocks that were metamorphosed to
165 upper greenschist – lower amphibolite facies at 2.69 Ga with some reaching granulite facies at
166 2.65 Ga (Krogh et al., 1984). CCS is located in a radial offset quartz-diorite dyke in the South
167 Range with brecciated country rocks and abundant sulfide mineralization (Lightfoot and Farrow,
168 2002) related to the ~1.85 Ga bolide impact. Post-impact thermal influences by multiple
169 orogenies, such as the Yavapai-Mazatzal (1.7-1.6 Ga), the Chieflakian-Pinwarian (1.5-1.4 Ga)
170 and the Grenville (1.2-1.0 Ga), have been found at various degrees across the Sudbury region,
171 e.g., mid- to upper-greenschist facies in the South Range (Fleet et al., 1987) and sub-greenschist
172 facies (< 150 ºC) in the North Range (Thompson et al., 1998).

173 The Thompson nickel belt (near Thompson, Manitoba) is a northeast-southwest trending
174 belt formed in an early Proterozoic continental margin. It is constituted by reworked Archean
175 basement and meta-supracrustal rocks (Hulbert et al., 2005). In the western part of the belt where
176 BT and TH are located, the rocks are dominated by 2.2 – 2.0 Ga serpentinized ultramafic rocks,
177 metagabbros, amphibolites, gneisses, schists, skarns, and quartzites (Hulbert et al., 2005;

178 Zwanzig et al., 2007). The rocks experienced a series of metamorphic events during 1850 – 1750
179 Ma (Couëslan et al., 2013) with peak metamorphic temperatures of ~ 700 ºC in the Thompson
180 area (Paktunç, 1984). Later (not yet dated) low-temperature (250 – 300 ºC) alteration of rocks at
181 Thompson by chloride-rich fluid is evidenced by the PGE-Au-As mineralization (Chen et al.,
182 1993).

183 Gas samples were collected following the method described by Ward et al. (2004) and
184 Holland et al. (2013). In brief, a packer was used to seal the borehole and funnel the water and
185 gas flow from the borehole through a sterilized Tygon tube into a bucket. After a period of
186 flushing to ensure representative sampling, gases were introduced into an inverted beaker
187 submerged into the fracture fluids collected in a bucket. The gases were then transferred through
188 a 22-g syringe needle on a Luer attachment at the top of the beaker into 160 ml borosilicate vials
189 with blue butyl stoppers which had been sterilized, prefixed with 50 μL saturated $HgCl_2$ solution,
190 and pre-evacuated.

191 Rocks samples were collected from exploration drill cores provided by the mines. A total
192 of 23 samples were selected from representative lithologies of the host rocks from KC, Sudbury,
193 and Thompson.
194

195 ## 3. Methods

196 Gas concentrations and nitrogen isotope compositions of N_2 were analyzed at University
197 of Toronto. Gas concentrations were generally measured within days after sample collection to
198 avoid possible shifts in gas (e.g., H_2 and O_2) concentrations due to diffusion and/or reaction,
199 although the results of re-analyses in 2007 on a batch of samples collected in 2000 show no

200 significant difference in H_2 and O_2 concentrations in comparison with the results obtained in
201 2000. Gas concentrations were measured by a Varian gas chromatography equipped with Varian
202 Molecular Sieve 5A PLOT fused silica column and a micro-thermal conductivity detector
203 (μTCD) for H_2, He, N_2, CO_2, O_2, Ar and a flame ionization detector for alkanes following the
204 published protocols (e.g., Ward et al., 2004). NH_3 is not specially examined here because it
205 requires high pH condition to drive NH_3 from fluids to gas phases (e.g., Deng et al., 2018),
206 whereas the modeling based on the pH and temperature conditions of the studied fluid samples
207 suggests that NH_3 mostly concentrates in fluids and barely occurs in the gas phases (Li et al.,
208 2012). The 2σ analytical error is < 5% of the absolute concentrations based on repeated analyses
209 of lab standards and natural samples. The nitrogen isotopic ratio of N_2 was measured by gas
210 chromatography-isotope ratio mass spectrometry. An aliquot of a gas sample was taken by gas-
211 tight syringe from a sample bottle and injected into a Varian gas chromatography, in which a
212 slow flow rate of 1.2 ml/min was used for the carrier gas (ultrahigh-purity helium) to ensure the
213 separation of N_2 from other gas components such as H_2 and O_2. CO_2 and CO are not significant
214 interferences in this analysis because their natural abundances in the gas samples are below the
215 detection limit (< 0.01 vol%). A time window was set to allow N_2 but no other interference gases
216 to be carried into a Finnigan 252 isotope ratio mass spectrometer for isotopic measurements. The
217 isotopic ratios are reported using the δ notation ($\delta^{15}N = (^{15}N/^{14}N)_{sample}/(^{15}N/^{14}N)_{standard} - 1$), in
218 which "standard" is atmospheric N_2. All samples were measured in duplicate. Repeat analyses of
219 these samples and laboratory working standards cross-calibrated against international IAEA
220 nitrogen reference materials gave 2σ analytical errors better than 0.2‰.

221 Nitrogen isotopic ratios of rocks were measured at University of Alberta following the
222 method described by Li et al. (2021a). In brief, after removal of the surface by sawing, rock

chips from drill cores were ground into fine powders (< 200 mesh). For the graphite-bearing lens samples, nitrogen was measured on both bulk-rock samples and refractory reduced carbon residues following the extraction protocol of Eigenbrode and Freeman (2006). The powder samples were weighted and loaded into pre-cleaned one end-sealed quartz tube together with CuO reagents, pumped in a metal manifold, sealed under high vacuum, and combusted first at 1200 ºC for 30 min to 60 min (depending on lithology; see details in Li et al., 2021a) and then at 900 ºC overnight to completely release the fixed nitrogen in minerals. The sample tube was then cracked under high vacuum to release N_2, which was further cryogenically purified, quantified by a capacitance manometer, and carried by an ultrahigh-purity helium gas to a Thermo Finnigan MAT 253 for nitrogen isotopic measurements. The $\delta^{15}N$ values are reported relative to the atmospheric N_2. Repeat analyses of two standards (Low Organic Content Soil and High Organic Content Soil) from Elemental Microanalysis Ltd gave 2σ analytical errors better than 0.2‰ (Li et al., 2021a).

4. Results

4.1. Gas concentrations and $\delta^{15}N_{N2}$ values

The major gas concentrations and $\delta^{15}N$ values of N_2 are reported in Table 1. The results are briefly summarized below.

Twenty-five gas samples from KC are dominated by CH_4 (64 – 83 vol%) and other light n-alkanes (e.g., ethane, propane, butane; in total < 9 vol%). N_2 is the second most abundant gas component with concentrations varying from 4.5 vol% to 16.9 vol% and $\delta^{15}N$ values from 3.2‰ to 8.0‰ (Table 1). These isotopic values fall in the $\delta^{15}N$ range of 2.8‰ – 8.8‰ from a limited

245 set of KC samples in Montgomery (1994) and Labidi et al. (2020). H_2 gas was detected in all KC
246 samples except one, with variable concentrations from 0.3 vol% to 10.7 vol%.

247 Two gas samples from LR are also dominated by CH_4 (66 – 72 vol%) and N_2 (9 – 15
248 vol%) with $\delta^{15}N$ values of 6.5‰ and 7.4‰, respectively. Both samples contain H_2 (1.8 vol% and
249 3.6 vol%, respectively). All these features are similar to those of the KC samples.

250 Six gas samples from CCS (on the south rim of the Sudbury Basin) are characterized by
251 extremely high H_2 concentrations (10 – 58 vol%). CH_4 is the other major gas component in these
252 samples (14 – 70 vol%). N_2 concentrations are generally low in the samples studied at this site
253 (Table 1). The $\delta^{15}N_{N2}$ values (0.6‰ to 4.2‰) of these samples are also much lower than those of
254 the KC and LR samples. It is worth noting that variable amounts of O_2 (0.4 – 5.5 vol%) are
255 detected in these samples, which suggests significant air contamination (see Section 4.2). In a
256 previous unpublished study by Montgomery (1994), much higher N_2 concentrations of up to 65
257 vol% and $\delta^{15}N$ values up to 17.5‰ were reported from CCS. The other samples from the
258 Sudbury Basin show significantly higher N_2 concentrations. The five NR gas samples are
259 dominated by N_2 (47 – 53 vol%), He (24 – 32 vol%) and CH_4 (15 – 24 vol%). H_2 occurs all
260 samples in varying amounts (0.01 – 2.7 vol%). The $\delta^{15}N_{N2}$ values display a small range from
261 3.5‰ to 5.0‰. The only gas sample available from FR is also dominated by N_2 (66 vol%), He
262 (17 vol%) and CH_4 (20 vol%). It also contains much higher Ar concentration (5.2 vol%) than all
263 the other studied gas samples from the Canadian Shield (< 2 vol%). The reason for this is not
264 fully understood at this time. The FR sample has a $\delta^{15}N_{N2}$ value of 5.0‰, similar to those of the
265 NR samples.

Three gas samples from BT and four gas samples from TH are all dominated by CH_4 and N_2. The CH_4 concentrations (63 – 69 vol%) are higher than N_2 concentrations (29 – 31 vol%) in the BT samples, whereas the N_2 concentrations (46 – 66 vol%) are higher than the CH_4 concentrations (35 – 48 vol%) in the TH samples. Despite the difference in N_2 concentration, the $\delta^{15}N_{N2}$ values are consistent between BT and TH, ranging from 7.4‰ to 8.7‰. All of the BT and TH gas samples except one contain detectable H_2, generally at levels between 0.02 – 2.75 vol%.

4.2. Distinguishing sampling-related air contamination

A characteristic feature of the studied gas samples from the Canadian Shield is the ubiquitous occurrence of H_2 gas (Table 1). This indicates that highly reducing conditions have been established and maintained in the host fracture fluids of these gas samples, which is consistent with all past studies. These highly reduced fracture fluids should not contain any *in-situ* O_2 gas (Holland et al., 2013; Warr et al;, 2018, 2021a). Therefore, any O_2 detected in the gas samples should be indicative of recent air contamination, mostly likely during sampling.

To assess the air contamination in the studied samples, $\delta^{15}N_{N2}$ values are compared with N_2/O_2 and N_2/Ar concentration ratios (Fig. 2). Fig. 2A illustrates a decreasing trend of $\delta^{15}N_{N2}$ values following the decrease in N_2/O_2 ratios toward the air end-member, particularly seen in some of the CCS and KC samples. The data comparison (Fig. 2A) shows that more consistent ranges of $\delta^{15}N_{N2}$ values can be observed for samples with N_2/O_2 ratios > 15 at each site. The $\delta^{15}N_{N2}$ values of samples with N_2/O_2 < 15 are more or less altered by air contamination.

Unlike O_2, which can be readily identified as a result of air contamination in these highly reducing fluids, ^{40}Ar (the dominant isotope of Ar) can be produced by subsurface processes and hence cannot be used to evaluate air contamination (Fig. 2B). ^{40}Ar, a product of the radioactive

289 decay of ^{40}K, can accumulate in the fracture waters over time and vary significantly depending
290 on the lithology of local host rocks and isolation time of the fracture fluids (Warr et al., 2019).
291 N_2 concentrations may also vary significantly, depending on the thermal history, nitrogen source,
292 abiotic reactions, and biological activities (if any) in the fracture waters (Silver et al., 2012).
293 These two factors can result in highly heterogeneous N_2/Ar ratios in the deep subsurface of the
294 Canadian Shield (Fig. 2B), which may be a result of *in-situ* processes and not necessarily reflect
295 air contamination. The data compilation of less contaminated samples (i.e., N_2/O_2 >15) on Fig.
296 2C illustrates that the N_2/Ar ratios increase in order from LR, FR, NR, KC, to BT and TH.
297 Therefore, without knowing the N_2/Ar values of uncontaminated gases, N_2/Ar ratios alone cannot
298 be used to estimate the fractions of air components in gas samples from Precambrian cratons.
299 Accordingly, the discussion below on the $\delta^{15}N_{N2}$ values of the Canadian Shield samples
300 will focus only on those with N_2/O_2 > 15.
301
302 **4.3. $\delta^{15}N$ values of rock samples**
303 The nitrogen concentrations and $\delta^{15}N$ values of rock samples are listed in Table 2.
304 Six silicate host rock samples from KC, including three rhyolites, two silicified cherty
305 breccia and one quartz feldspar porphyry, show a $\delta^{15}N$ range from 6.0‰ to 10.4‰. Six samples
306 of the graphite-bearing lenses from KC give a $\delta^{15}N$ range from 6.7‰ to 15.6‰ for bulk-rock
307 nitrogen, but a lower $\delta^{15}N$ range from 0.4‰ to 10.4‰ for extracted refractory reduced carbon
308 residues.
309 Sudbury host rock samples comprise of two samples (a meta-gabbro and a breccia
310 matrix) from the Creighton mine, which has similar wall rock to the CCS mine, and six samples
311 from NR (two felsic gneisses, two felsic norites, one granodiorite, and one breccia). All the

312 samples give a small $\delta^{15}N$ range from 1.3‰ to 3.4‰ except one felsic norite sample with a $\delta^{15}N$
313 value of -5.6‰.
314 Three host rock samples from TH, inducing one gneiss, one schist, and one skarn, show
315 relatively high $\delta^{15}N$ values from 7.0‰ to 10.2‰.
316

317 # 5. Discussion

318 ## 5.1. $\delta^{15}N_{N2}$ variability across sites in the Canadian Shield

319 After discarding all the samples with $N_2/O_2 < 15$, the $\delta^{15}N_{N2}$ distribution (Fig. 2C) shows
320 a general trend with the lowest values in NR and FR, and steadily increasing values from LR,
321 KC, to BT and TH. However, this isotopic pattern is not confirmative at the moment given that
322 only a small number of samples were collected from a specific depth in each of the sites (except
323 KC). A larger dataset from multiple depths at KC give much larger $\delta^{15}N_{N2}$ variation than those of
324 the other sites (Fig. 2C; see Section 5.4 for discussion). Two samples from different depths at
325 CCS also show large $\delta^{15}N_{N2}$ variation (Montgomery, 1994; Fig. 2A). Therefore, more data from
326 each site are needed in future studies to examine the inter-site $\delta^{15}N_{N2}$ variability and its
327 controlling factors in the Canadian Shield.
328

329 ## 5.2. Comparison with the Fennoscandian Shield and the Kaapvaal Craton

330 The $\delta^{15}N$ values of N_2 from subsurface fracture fluids have been reported from some sites
331 on other Precambrian cratons, e.g., the Fennoscandian Shield (Sherwood Lollar et al., 1993a) and
332 the Kaapvaal Craton (Silver et al., 2012). As mentioned above, the thirteen published gas
333 samples from the Fennoscandian Shield (Sherwood Lollar et al., 1993a) have $\delta^{15}N_{N2}$ values from
334 0.2‰ to 5.1‰ (except one high value of 10.0‰) with a peak at the bin of 0-1‰ (Fig. 3A). Silver

et al. (2012) reported the $\delta^{15}N_{N2}$ values of eighteen gas samples from Beatrix (BE116, 325, 327), Driefontein (Dr938), Evander (EV219, 522, 818), Kloof (KL441, 739), Masimong (MM5), Merriespruit (MS151), Mponeng (MP104) in the Witwatersrand Basin in the Kaapvaal Craton. These fracture systems have mean residence times varying from 0.7 Ma (EV522) to 20 Ma (KL739 and MP104) with one sample (Dr938) having a ^{14}C-derived age of 1022 years (Lippmann et al., 2003; Lin et al., 2006; Silver et al., 2012 and reference therein). The hydrogen and oxygen isotope compositions of these fracture fluids spread from on (or close to) the global meteoric water line (GMWL) to above the GMWL (Lippmann et al., 2003; Ward et al., 2004; Lin et al., 2006; Onstott et al., 2006; Warr et al., 2021a). Their $\delta^{15}N_{N2}$ values fall in the range of –1.3‰ to 5.8‰ (Fig. 3B). The $\delta^{15}N_{N2}$ values do not correlate with either the residence times or the magnitude of isotopic deviation above the GMWL, indicating the major control on the $\delta^{15}N_{N2}$ values of the samples in the Kaapvaal Craton may not be geological processes (e.g., fluid-rock interaction) but biological processes.

In contrast, the Canadian Shield samples show consistently higher $\delta^{15}N_{N2}$ values (Fig. 3C). A total of thirty-five samples studied here cluster in a $\delta^{15}N_{N2}$ range of 3.0‰ to 8.0‰ with a peak at the bin of 7–8‰ (Fig. 3C), while three historical samples from Montgomery (1994) and Sherwood Lollar (1993a) give more variable $\delta^{15}N_{N2}$ values of 1.4‰, 1.5‰ and 17.5‰, respectively (Fig. 2A). The $\delta^{15}N_{N2}$ discrepancy between the Canadian Shield samples and the samples from the Fennoscandian Shield and the Kaapvaal Craton could be attributed to the differences in nitrogen source and abiotic and biological processes among these deep subsurface fracture waters, which are discussed in detail below.

5.3. Source of N_2 in the Canadian Shield

Several sources could potentially contribute to the N_2 in the terrestrial subsurface fracture water systems, such as ancient atmospheric N_2, dissolved inorganic nitrogen species (nitrate, nitrite, ammonium) in pore water and/or fluid inclusions in host rocks, and fixed nitrogen in host rocks.

In the studied samples from the Canadian Shield, although noble gas studies imply that these fracture fluids contain a minor initial component of noble gas (e.g., Xe) derived from ancient air (Holland et al., 2013; Warr et al., 2018), a ballpark estimation based on the concentration data of gases and rocks in Li et al. (2016) and typical N_2 concentration of seawater (Kipfer et al., 2002) suggests that the ancient air contributed at most 0.1 – 6% of the gas components. Therefore, ancient atmospheric N_2 can be excluded as the main source. In addition, a recent study discovered extreme $^{15}N^{15}N$ enrichment of atmospheric N_2 (Yeung et al., 2017). Assuming the ancient atmospheric N_2 had comparable $^{15}N^{15}N$ enrichment, and little re-ordering of the internal bonding of N_2 molecules in these low-temperature fracture systems, a $^{15}N^{15}N$ enrichment would be expected if significant amount of ancient atmospheric N_2 contributed to the fluids. However, Labidi et al. (2020) found no $^{15}N^{15}N$ enrichment in the KC samples. This suggests that the amounts of atmospheric N_2, from both ancient air and modern air contamination, are relatively small in the total N_2 of the samples.

Dissolved inorganic nitrogen species in pore water and fluid inclusions in host rock have been proposed to account for the abundant nitrate, N_2 and ammonium in the subsurface fracture waters in the Witwatersrand Basin in the Kaapvaal Craton, South Africa (Silver et al., 2012). In this model, it requires (1) a high NH_3-NH_4^+ pool in fluid inclusions in the first place, (2) efficient migration of nitrogen in fluid inclusions to fracture fluids, and (3) abiotic and biological recycling processes to convert NH_3/NH_4^+ to other nitrogen species (e.g., N_2 in this case). These

conditions are relatively difficult to reach in the Canadian Shield where the igneous-rock dominated host rocks contain small volumes of primary fluid inclusions. Furthermore, geochemical and hydrogeological analyses have shown that contribution of young surface fluids is little in these fracture systems (e.g., Warr et al., 2021a), ruling out later infiltration of dissolved inorganic nitrogen from surface.

Sedimentary rocks are a commonly considered source for N_2 in basinal environments. However, in the Canadian Shield, host rocks are dominated by crystalline rocks. At KC where host rock lithology has been well characterized from drill cores, graphite-bearing lenses occupy a very small volume in host rocks. The nitrogen concentrations of the graphite-bearing lenses (40-99 ppm; Table 2) are significantly smaller than those of typical deep-sea sediments and their metamorphosed equivalents (hundreds to thousands of ppm; e.g., Bebout and Fogel, 1992; Busigny et al., 2003; Sadofsky and Bebout, 2004; Li and Bebout, 2005). Therefore, the graphite-bearing lenses can less likely account for the widely occurring gases in the highly confined and locally controlled fracture water compartments (Warr et al., 2018). This conclusion is further supported by the carbon and hydrogen isotopic signatures of n-alkanes in the gas samples. The $\delta^{13}C$ and $\delta^{2}H$ patterns of n-alkanes are very different to that of conventional thermogenic gases (Sherwood Lollar et al., 1993b, 2002, 2008; Warr et al., 2021b). Overall, both isotopic fingerprints and hydrogeological frameworks do not favor organics as the main source of the gases.

Significant amounts of nitrogen (in form of ammonium) can be assimilated into the crystal structures of secondary phyllosilicate minerals (e.g., clay and serpentine) formed during the alteration of igneous rocks by seawater and/or hydrothermal fluids (Busigny et al., 2005; Li

et al., 2007). The nitrogen measurement on six representative silicate samples from KC give a nitrogen concentration range from 12 ppm to 34 ppm (average: ~ 24 ppm; Table 2) and a $\delta^{15}N$ range from 6.0‰ to 10.3‰ (average: 8.0‰). Given the large volume of the silicate host rocks in Precambrian cratons, such high nitrogen concentrations of the igneous host rocks represent a huge nitrogen reservoir, with an inventory orders in magnitude higher than that in the small volume of fluids. Mobilization by devolatilization of a small proportion of this reservoir is able to account for the N_2 in the subsurface fracture waters.

To devolatilize the ammonium fixed in the igneous host rocks, it requires relatively high temperatures. In light of previous laboratory and field studies (e.g., Haendel et al., 1986; Bebout and Fogel, 1992), nitrogen devolatilization from minerals and rocks could have easily taken place under the peak (and retrograde) metamorphic conditions in the study sites, e.g., 400 ºC at KC, 700 ºC at TH, and variable temperatures (depending on the distance to the crater; Abramov and Kring, 2004) during the impact event at Sudbury. At crustal conditions, high temperatures facilitate N_2 as the devolatilization product (e.g., Bebout and Fogel, 1992; Li et al., 2009). The lower temperature limit for N_2 devolatilization from minerals and rocks is however unconstrained. Even taking the smectite-illite transition temperature of 60 ºC (Freed and Peacor, 1989) as the lower limit, it is still higher than the current temperatures of the studied fracture fluid systems. In particular, the Canadian Shield has been relatively stable and maintained a low thermal gradient since at least 2 Ga (Slack, 1974). Temperature estimation using the method of Li et al. (2016) suggests that the temperature at KC should have been < 60 ºC since at latest 1.3 Ga for the 2.1 kmbs site and 0.9 Ga for the 2.9 kmbs site. Therefore, the observed N_2 was mostly likely produced during earlier time periods. N_2 production would have been most efficient during the peak metamorphism at each site, and diminish exponentially with the decrease in temperature

with time. Given that the analyzed host rocks consistently show high nitrogen concentrations (Table 2), it only requires a very small (almost negligible) fraction of the total nitrogen in the rocks to account for the observed N_2 in the fluids, which can be easily satisfied.

5.4. Possible N recycling processes in subsurface fracture fluids

5.4.1. Abiotic N_2 reduction

Based on above discussions, the N_2 in the deep subsurface fracture fluids in the Canadian Shield most likely originated by devolatilization of fixed ammonium in their silicate host rocks. Nitrogen devolatilization from rocks is associated with an isotopic effect with preferential uptake of ^{14}N by N_2 and preferential retention of ^{15}N in host rock (e.g., Bebout and Fogel, 1992; Haendel et al., 1986; Li et al., 2021b, c). The magnitude of ^{15}N depletion in the N_2 product is dependent on two factors, i.e., the temperature-dependent isotope fractionation factor and the fraction of ammonium in rock that is converted into N_2. The nitrogen isotope fractionation factors between N_2 and clay minerals can be derived from Li et al. (2021b, c) to be –13.2‰ at 60 ºC, –10.9‰ at 100 ºC, –6.2‰ at 200 ºC,–4.1‰ at 400 ºC, –2.3‰ at 700 ºC and –1.5‰ at 1000 ºC. Based on these fractionation factors, the theoretical $\delta^{15}N$ differences between N_2 product and remaining ammonium in host rocks along the progress of metamorphic devolatilization are illustrated by a Rayleigh fractionation model in Fig. 4A-C for KC, Sudbury and Thompson, respectively. Comparison of average $\delta^{15}N$ values between N_2 and host rocks yield $\Delta^{15}N_{N2\text{-}rock}$ values of –0.3‰ for the 2.1 kmbs site, –1.1‰ for the 2.4 kmbs site, and –3.1‰ for the 2.9 kmbs site at KC, +2.5‰ at NR, +4.0‰ at FR, +0.3‰ at TH and –0.4‰ at BT. All these values are higher than the expected values for N_2 devolatilization at their peak metamorphic conditions (Fig. 4A-C). Any N_2 generated from retrograde metamorphism would make the isotope discrepancy ever larger. At CCS, although all the samples in this study have been severely

449 contaminated by air during sampling, their values are still higher than the predicted values (Fig.
450 4B), not even mention the extremely high $\delta^{15}N$ values (up to 17.5‰) observed on less air-
451 contaminated samples (Montgomery, 1994). These results indicate, while the magnitude and
452 direction of isotope fractionation are indeed consistent with N_2 production via devolatilization of
453 ammonium in host rocks, the extents of observed isotopic discrepancy between N_2 and host
454 rocks require an additional process to explain the ^{15}N enrichments in N_2.

455 Diffusive loss of N_2 and abiotic N_2 reduction are two known processes that can induce
456 ^{15}N enrichments in remaining N_2. Extensive studies of the noble gas concentrations (in the KC
457 system in particular) have demonstrated that diffusion cannot be a major factor due to the
458 concordance in the ages of the fluids derived from both light (helium and neon) and heavy (argon
459 and xenon) noble gases. In systems where diffusion is a significant process, preferential loss of
460 light noble gases would produce an artifact of significantly younger apparent ages for helium and
461 neon – which is notably not observed in any of the KC studies (Holland et al., 2013; Warr et al.,
462 2018). Accordingly, diffusion process is less likely to significantly impact the $\delta^{15}N_{N2}$. Rather
463 than diffusion, abiotic N_2 reduction may play an important role. Following the cooling of the
464 fluids, N_2 input from metamorphic devolatilization diminished to negligible level. Meanwhile,
465 the nonstop interaction between water and Fe^{2+}-bearing minerals (e.g., olivine, pyroxene, biotite,
466 pyrite) in host rocks can produce secondary minerals to seal the fracture system and subsequently
467 establish and maintain a highly reducing environment enriched in H_2 and dissolved Fe^{2+} (Li et
468 al., 2016) inside the fracture system. These reducing agents in the fuids, as well as abundant
469 Fe^{2+}-bearing minerals in host rocks, would facilitate abiotic reduction reactions. This is
470 supported by the observation that abiogenic products (e.g., alkanes, acetate, and formate)
471 dominate the gaseous and/or dissolved organic compounds in the KC fracture fluids (Sherwood

Lollar et al., 2021) and also widely occur (if not dominate) in other sites in the Canadian Shield (Sherwood Lollar et al., 2006).

Abiotic N_2 reduction in a geological setting generally refers to the mineral catalyzed reduction of N_2 to produced NH_3 or NH_4^+ in fluids, via reactions such as equation (1):

$$N_2 + 6Fe^{2+} + 8H^+ \rightarrow 2NH_4^+ + 6Fe^{3+} \quad (1)$$

Laboratory experiments demonstrate that abiotic N_2 reduction is most efficient at 500 ºC (Brandes et al., 1998), but can also occur at temperatures as low as 22 ºC (Smirnov et al., 2008). Abiotic N_2 reduction generally produces a kinetic nitrogen isotopic effect due to the difficulty in breaking the strong N≡N bond of N_2. Based on the nitrogen isotopic measurements of altered igneous rocks, Li et al. (2007, 2014) yielded nitrogen isotopic enrichment factors of –15‰ to –11‰ for abiotic N_2 reduction at medium- to high-temperature hydrothermal conditions (>300 ºC). The magnitude of kinetic nitrogen isotopic effect could be larger at lower temperatures (Li et al., 2009), but no data are available yet. Using the average value of -13‰ (Li et al., 2007, 2014) as the lower limit and a Rayleigh fractionation model (Fig. 4D-F), a ballpark estimate can be made for the fractions of N_2 required to be reduced in order to match the observed $\delta^{15}N$ value in the studied samples. The results suggest that the fractions of the initial N_2 that has been abiotically reduced is 25 – 63% at 2.1 kmbs, 21 – 61% at 2.4 kmbs, and 7 – 54% at 2.9 kmbs, respectively (Fig. 4D). This decreasing trend along depth is self-consistent with the temperature and time framework that 2.1 kmbs has the shortest time for N_2 production but longest time and lowest temperature for abiotic N_2 reduction, whereas the 2.9 kmbs has the longest time for N_2 production but shortest time and highest temperature for abiotic N_2 reduction. Similar extents of abiotic N_2 reduction are also obtained from NR (27 – 70%), FR (35 – 74%), TH (18 – 65%), and

494 BT (14 – 63%) (Fig. 4 E, F). Future examinations on concentrations and isotope compositions of
495 ammonium in the fluids may help to test this possibility.
496 It is worth noting that, based on mass balance and isotopic comparison, Silver et al.
497 (2012) also proposed that abiotic N_2 reduction could have occurred in the subsurface fracture
498 fluids in the Kaapvaal Craton. This implies that abiotic N_2 reduction might occur widely in
499 Precambrian cratons.
500
501 **5.4.2. The role of radiolysis?**
502 Another process that is worth briefly discussing is radiolysis. Energy released from the
503 decay of radioactive isotopes of K, U, Th in host rocks has been shown to play an important role
504 in the long-term production of deep subsurface hydrogen (e.g., Lin et al., 2005; Sherwood Lollar
505 et al., 2014), carbon (Sherwood Lollar et al., 2021), and sulfur (Lin et al., 2006; Li et al., 2016)
506 in deep fracture fluids in the Precambrian cratons around the world. An intriguing question is
507 how much this process may contribute to the nitrogen cycle in these deep saline fracture fluids.
508 Silver et al. (2012) carried out laboratory experiments to irradiate NH_3/NH_4^+ in anaerobic
509 solutions and observed production of nitrite and nitrate. Consequently, radiolysis has been
510 proposed to be part of the multiple abiotic and biotic mechanisms to drive the nitrogen cycle in
511 the subsurface fluids in the Kaapvaal Craton (Silver et al., 2012). Radiolytic impact on fixed
512 ammonium in minerals and rocks is poorly examined by far. It is unclear whether radiolysis in
513 the Precambrian cratonic environments facilitate N_2 production. But laboratory experiments on
514 the N_2-H_2-H_2O system (e.g., Etoh et al., 1987; Karasawa et al., 1991) have demonstrated that N_2
515 can be consumed by radiolysis to form not only NH_4^+ as the dominant product (Karasawa et al.,
516 1991) but also NO_3^- (Etoh et al., 1987), via overall reactions described in equations (2)-(3).

$$\begin{cases} N_2 \xrightarrow{radiation} N^{\cdot} + N^{\cdot} \\ H_2O \xrightarrow{radiation} H^{\cdot} + O^{\cdot} \end{cases} \quad (2)$$

$$\begin{cases} N^{\cdot} + 3H^{\cdot} + H^{+} \longrightarrow NH_4^{+} \\ 2N^{\cdot} + 5O^{\cdot} + 2OH^{-} \longrightarrow 2NO_3^{-} + H_2O \end{cases} \quad (3)$$

This differs from the mineral catalyzed abiotic N_2 reduction process in equation (1). However, the nitrogen isotope fractionation during radiolytic decomposition of N_2 has not been constrained, although a kinetic isotopic effect likely occurs. Future studies integrating laboratory examination of nitrogen isotope fractionations during radiolysis of the N_2-H_2-H_2O system and the analyses of concentrations and isotope compositions of ammonium and nitrate (if there is any) in fracture fluids are necessary to further assess these processes in the deep subsurface of Precambrian cratons.

5.4.3. Microbial nitrogen recycling?

The samples studied here contain a set of N_2 samples from one of the long-term monitoring boreholes (BH12299 at 2.4 kmbs) at the KC Observatory collected over nearly 10 years since the completion of the borehole drilling in May 2007. Interestingly, the $\delta^{15}N_{N2}$ values of this set of samples (Table 1) display a trend of steady decrease (for >1‰) over time (Fig. 5). Since significant addition of an air component over time can be ruled out based on the $^{15}N^{15}N$ results (Labidi et al., 2020), this trend suggests that another *in-situ* source of ^{15}N-depleted N_2 has been progressively added into the original N_2 reservoir in this borehole over the monitoring period. Although the N_2 in the deeper fracture fluids (e.g., 2.9 kmbs) at the KC Observatory is relatively ^{15}N depleted, it cannot be the source for the 2.4 kmbs fracture fluids because current evidence supports hydrogeologic isolation between these fracture systems (Warr et al., 2018, 2021b). One potential *in-situ* source for a ^{15}N-depleted N_2 source in the 2.4 kmbs fracture system

539 is dissolved ammonium. The temperature and pH conditions of the KC fluids favor the
540 preservation of ammonium as the net product from abiotic N_2 reduction (Li et al., 2012). This
541 may therefore provide an ideal ^{15}N-depleted source for this secondary N_2.
542 The abiotic conversion of NH_4^+/NH_3 to N_2 requires either oxic condition and/or relatively
543 high temperature (>500 ºC) without catalyst (Li et a., 2009). Even with efficient catalyst (e.g.,
544 Fe), the conversion rate is very slow at temperatures < 300 ºC (Li et al., 2021d). In addition, no
545 evidence to show an oxic environment in the studied fracture systems. Thus, abiotic conversion
546 of NH_4^+/NH_3 at the low-temperature environment (24 ºC at 2.4 kmbs) may not contribute
547 detectable N_2 to BH12299 fluid at a decadal time scale. Microbially-driven anaerobic oxidation
548 of ammonium (e.g., Van De Graaf et al., 1995; Byrne et al., 2008) is a more efficient mechanism
549 to convert ammonium to N_2. Microbial recycling of nitrogen has been suggested to occur in
550 subsurface fracture fluids in the Kaapvaal Craton (Silver et al., 2012; Lau et al 2016) and
551 elsewhere in the Canadian Shield (Sheik et al., 2021), but cannot be explored further for the KC
552 samples due to the lack of biogeochemical data and isotopic compositions of other nitrogen
553 species (ammonium, nitrite or nitrate, if there is any) in these fracture fluids. It is worth
554 highlighting though that recent studies using cell counts and culture-based methods have
555 identified low abundance of H_2-utilizing, alkane-oxidizing sulfate-reducing bacteria in the KC
556 fracture fluids (Lollar et al., 2019; Wilpiszeski et al., 2020). This directly supports the prevailing
557 hypothesis that microbial activities could have been sustained over geological timescale in the
558 long isolated KC fracture fluids based on sulfur isotopic studies (Li et al., 2016). Microbial
559 activities related to methanogenesis and methanotrophy in the 2.4 kmbs KC fracture fluids have
560 been further inferred from the isotopic signatures of CH_4 (Sherwood Lollar et al., 2002; Young et
561 al., 2017, Warr et al., 2021b). In particular, a potential ongoing addition of biogenic CH_4 to the

same fracture fluid system (BH12299) has been suggested based on a temporal decrease in the mass-18 isotopologues of CH_4 over the last decade (Warr et al., 2021b). A speculation is that the KC fracture fluids could have been or is being influenced by microbial activities involving multiple metabolic pathways including H_2 oxidation, sulfate reduction, methanogenesis, anaerobic oxidation of methane, and anaerobic oxidation of ammonium. This hypothesis will need to be tested by future microbial studies with detailed constraints on metabolic pathways and their geochemical fingerprints.

6. Conclusions

N_2 in the highly reducing saline fracture waters of the Canadian Shield provides a novel opportunity to look into the (bio)geochemical nitrogen recycling processes in deep subsurface systems that have been long investigated in the context of the deep carbon cycle and subsurface life, but to date with very little characterization and quantification of the deep nitrogen cycle. Here we observed that the N_2 in subsurface fracture waters with residence times from hundreds of million years to billions of years in the Canadian Shield were more enriched in ^{15}N than the N_2 samples from fracture waters with residence times of hundreds of thousands to tens of millions of years in the Fennoscandian Shield and the Kaapvaal Craton. Detailed isotopic comparison between the Canadian Shield N_2 samples and their potential sources excludes air, dissolved inorganic nitrogen, and organic compounds in host rocks as their sources. Instead, fixed ammonium in igneous host rocks is the most likely source. Modeling of nitrogen devolatilization of igneous rocks supports this interpretation, but also suggests that a second process is required to account for the observed ^{15}N enrichments in the N_2 samples from the Canadian Shield. Long-term abiotic N_2 reduction in the closed fracture water systems is the most likely process. The

585 data in this study imply a common occurrence of abiotic N_2 reduction in the long isolated, highly
586 reducing fracture water systems in the Canadian Shield, and possibly in similar environments on
587 the early Earth and other planets. The accumulation of the ammonium product can not only
588 provide a critical reagent for abiotic synthesis of amino acid (an essential building block for life)
589 toward the origin of life but also supply a necessary nutrient to support potential ammonium
590 assimilating or anaerobic ammonium oxidizing microbes in these environments.

591

592 ## Acknowledgements

593 This study was partially supported by NSERC and Canada Research Chair funding to
594 BSL and NSERC Discovery grant to LL. BSL is a Fellow and Co-Director for the CIFAR Earth
595 4D program in subsurface science and exploration. We thank Thomas Eckert and Scott Mundle
596 for field assistance and Georges Lacrampe-Couloume for lab assistance. Thanks are due to
597 colleagues and supporters at the mines whose efforts and support for the sampling program were
598 invaluable. This manuscript benefited from constructive comments by Dr. Eva Stüeken and an
599 anonymous reviewer.

600

601 ## References

602 Abramov, O., Kring, D.A., 2004. Numerical modeling of an impact-induced hydrothermal
603 system at the Sudbury crater. J. Geophys. Res., 109: E10007.
604 Doi:10.1029/2003JE002213.
605 Barrie, C.T., Davis, D.W., 1990. Timing of magmatism and deformation in the Kamiskotia-Kidd
606 Creek area, western Abitibi Subprovince, Canada. Precam. Res., 46: 217-240.
607 Bebout, G.E., Fogel, M.L., 1992. Nitrogen-isotope compositions of metasedimentary rocks in the
608 Catalina Schist, California: implications for metamorphic devolatilization history.
609 Geochim. Cosmochim. Acta, 56: 2839-2849.

610 Bleeker, W., Parrish, R.R., 1996. Stratigraphy and U-Pb zircon geochronology of Kidd Creek:
611 implications for the formation of giant volcanogenic massive sulphide deposits and the
612 tectonic history of the Abitibi greenstone belt. Can. J. Earth Sci., 33: 1213-1231.
613 Brandes, J.A., Boctor, N.Z., Cody, G.D., Cooper, B.A., Hazen, R.M., Yoder Jr, H.S., 1998.
614 Abiotic nitrogen reduction on the early Earth. Nature, 395: 365-367.
615 Busigny, V., Cartigny, P., Philippot, P., Ader, M., Javoy, M., 2003. Massive recycling of
616 nitrogen and other fluid-mobile elements (K, Rb, Cs, H) in a cold slab environment:
617 evidence from HP to UHP oceanic metasediments of the Schistes Lustrés nappe (western
618 Alps, Europe). Earth and Planetary Science Letters, 215: 27-42.
619 Busigny, V., Laverne, C., Bonifacie, M., 2005. Nitrogen content and isotopic composition of
620 oceanic crust at a superfast spreading ridge: a profile in altered basalts from ODP Site
621 1256, Leg 206. Geochem. Geophys. Geosyst., 6: Q12O01.
622 Byre, N., Strous, M., Crépeau, V., Kartal, B., Birrien, J.-L., Schmid, M., Lesongeur, F.,
623 Schouten, S., Jaeschke, A., Jetten, M., Prieur, D., Godfroy, A., 2008. Presence and
624 activity of anaerobic ammonium-oxidizing bacteria at deep-sea hydrothermal vents. The
625 ISME J., 3: 117-123.
626 Chen, Y., Fleet, M.E., Pan, Y., 1993. Platinum-group minerals and gold in arsenic-rich ore at the
627 Thompson Mine, Thompson Nickel Belt, Manitoba, Canada. Mineral. Petrol., 49: 127-
628 146.
629 Couëslan, C.G., Pattison, D.R.M., Dufrane, S.A., 2013. Paleoproterozoic metamorphic and
630 deformation history of theThompson Nickel Belt, Superior Boundary Zone, Canada, from
631 in situ U–Pb analysis of monazite. Precam. Res., 237: 13-35.
632 Davis, D.W., 2008. Sub-million-year age resolution of Precambrian igneous events by thermal
633 extraction–thermal ionization mass spectrometer Pb dating of zircon: Application to
634 crystallization of the Sudbury impact melt sheet. Geology, 36: 383-386.
635 Davis, D.W., Schandl, E.S., Wasteneys, H.A., 1994. U-Pb dating of minerals in alteration halos
636 of Superior Province massive sulfide deposits: syngenesis versus metamorphism.
637 Contrib. Mineral. Petrol., 115: 427-437.
638 Deng, Y., Li, Y., Li, L., 2018. Experimental investigation of nitrogen isotopic effects associated
639 with ammonia degassing at 0–70° C. Geochim. Cosmochim. Acta, 226: 182-191.
640 Dimroth, E., Imreh, L., Goulet, N., Rocheleau, M., 1983. Evolution of the south-central part of
641 the Archean Abitibi belt, Quebec. Part II: Tectonic evolution and geomechanical model.
642 Can. J. Earth Sci., 20: 1355-1373.
643 Doig, F., Sherwood Lollar, B., Ferris, F.G., 1995. Evidence for abundant microbial communities
644 in Canadian Shield groundwaters – an in situ biofilm experiment. Geomicrob. J., 13: 91-
645 101.
646 Eigenbrode, J.L., Freeman, K.H., 2006. Late Archean rise of aerobic microbial ecosystems.
647 PNAS 103, 15759-15764.
648 Etoh, Y., Karasawa, H., Ibe, E., Sakagami, M., Yasuda, T., 1987. Radiolysis of N_2-H_2O systems.
649 J. Nuclear Sci. Techol., 24: 672-674.
650 Faggart, B.E., Basu, A.R., Tatsumoto, M., 1985. Origin of the Sudbury complex by meteoritic
651 impact: neodymium isotopic evidence. Science, 230: 436-439.
652 Fleet, M.E., Barnett, R.L., Morris, W.A., 1987. Prograde metamorphism of the Sudbury igneous
653 complex. Can. Mineral., 25: 499-514.
654 Frape, S.K., Fritz, P., McNutt, R.H., 1984. Water-rock interaction and chemistry of groundwaters
655 from the Canadian Shield. Geochim. Cosmochim. Acta, 48: 1617-1627.

Freed, R.L., Peacor, D.R., 1989. Variability in temperature of the smectite/illite reaction in Gulf Coast sediments. Clay Minerals, 24: 171-180.
Goodwin, A., 1996. Principles of Precambrian Geology. Academic Press, pp 327.
Haendel, D., Mühle, K., Nitzsche, H.-M., Stiehl, G., Wand, U., 1986. Isotopic variations of the fixed nitrogen in metamorphic rocks. Geochim. Cosmochim. Acta, 50: 749-758.
Hannington, M.D., Bleeker, W., Kjarsgaard, I., 1999. Sulfide mineralogy, geochemistry, and ore genesis of the Kidd Creek deposit: Part I. North, Central and South orebodies. In: Hannington, M.D., Barrie, C.T. (Eds.), The Giant Kidd Creek Volcanogenic Massive Sulfide Deposit, Western Abitibi Subprovince, Canada, pp. 163-224.
Heard, A.W., Warr, O., Borgonie, G., Linage, B., Kuloyo, O., Fellowes, J.W., Magnabosco, C., Lau, M.C.Y., Erasmus, M., Cason, E.D., van Heerden, E., Kieft, T.L., Mabry, J.C., Onstott, T.C., Sherwood Lollar, B., Ballentine, C.J., 2018. South African crustal fracture fluids preserve paleometeoric water signatures for up to tens of millions of years. Chem. Geol., 493: 379-395.
Hoffmann, P.F., 1989. Precambrian geology and tectonic history of North America. In: Bally, A.W., Palmer, A.R. (Eds.), The Geology of North America - An Overview. The Geological Society of America, pp. 447-512.
Holland, G., Sherwood Lollar, B., Li, L., Lacrampe-Couloume, G., Slater, G., Ballentine, C.J., 2013. Deep fracture fluids isolated in the crust since the Precambrian era. Nature, 497: 357-360.
Hulbert, L., Hamilton, M.A., Horan, M.F., Scoates, R.F.J., 2005. U-Pb zircon and Re-Os Isotope geochronology of mineralized ultramafic intrusions and associated nickel ores from the Thompson nickel belt, Manitoba, Canada. Econ. Geol., 100: 29-41.
Itävaara, M., Nyyssönen, M., Kapanen, A., Ahonen, L., Kukkonen, I.T., 2011. Characterization of bacterial diversity to a depth of 1500 m in the Outokumpu deep borehole, Fennoscandian Shield. FEMS Microbiol. Ecol., 77: 295-309.
Karasawa, H., Ibe, E., Uchida, S., Etoh, Y., Yasuda, T., 1991. Radiation induced decomposition of ntirogen. Int. d. Radiat. Appl. lnstrum. Part C Radiat. Phys. Chem., 37: 193-197.
Kietäväinen, R., Ahonen, L., Kukkonen, I.T., Niedermann, S., Wiersberg, T., 2014. Noble gas residence times of saline waters within crystalline bedrock, Outokumpu Deep Drill Hole, Finland. Geochim. Cosmochim. Acta, 145: 159-174.
Kipfer, R., Aeschbach-Hertig, W., Peeters, F. and Stute, M., 2002. Noble gases in lakes and ground waters. In: Noble Gases in Geochemistry and Cosmochemistry (eds., D. Porcelli, C.J. Ballentine and R. Wieler). Reviews in Mineralogy and Geo-chemistry. Mineralogical Society of America, pp. 615–700.
Krogh, T.E., McNutt, R.H., Davis, G.L., 1982. Two high precision U-Pb zircon ages for the Sudbury nickel irruptive. Can. J. Earth Sci., 19: 723-728.
Labidi, J., Barry, P.H., Bekaert, D.V., Broadley, M.W., B., M., Giunta, T., Warr, O., Sherwood Lollar, B., Fischer, T.P., Avice, G., Caracausi, A., Ballentine, C.J., Halldórsson, S.A., Stefánsson, A., Kurz, M.D., Kohl, I.E., Young, E.D., 2020. Hydrothermal 15N15N abundances constrain the origins of mantle nitrogen. Nature, 580: 367-374.
Lau, M.C.Y., Kieft, T.L., Kuloyo, O., Linage-Alvarez, B., van Heerden, E., Lindsay, M.R., Magnabosco, C., Wang, W., Wiggins, J.B., Guo, L., Perl,am, D.H., Kyin, S., Shwe, H.H., Harris, R.L., Oh, Y., Yi, M.J., Purtschert, R., Slater, G.F., Ono, S., Wei, S., Li, L., Sherwood Lollar, B., Onstott, T.C., 2016. An oligotrophic deep-subsurface community

dependent on syntrophy is dominated by sulfur-driven autotrophic denitrifiers. PNAS, 113: E7927-E7936.
Li, L. and Bebout, G.E., 2005. Carbon and nitrogen geochemistry of sediments in the Central American convergent margin: Insights regarding subduction input fluxes, diagenesis, and paleoproductivity. J. Geophys. Res., 110: B11202, doi:10.1029/2004JB003276.
Li, L., Bebout, G.E., Idleman, B.D., 2007. Nitrogen concentration and $\delta^{15}N$ of altered oceanic crust obtained on ODP Legs 129 and 185: insights into alteration-related nitrogen enrichment and the nitrogen subduction budget. Geochim. Cosmochim. Acta, 71: 2344-2360.
Li, L., Cartigny, P., Ader, M., 2009. Kinetic nitrogen isotope fractionation associated with thermal decomposition of NH_3: Experimental results and potential applications to trace the origin of N_2 in natural gas and hydrothermal systems. Geochim. Cosmochim. Acta, 73: 6282-6297.
Li, L., Sherwood Lollar, B., Li, H., Wortmann, U.G., Lacrampe-Couloume, G., 2012. Ammonium stability and nitrogen isotope fractionations for NH_4^+–$NH_{3(aq)}$–$NH_{3(gas)}$ systems at 20–70 ^oC and pH of 2–13: Applications to habitability and nitrogen cycling in low-temperature hydrothermal systems. Geochim. Cosmochim. Acta, 84: 280-296.
Li, L., Zheng, Y.-F., Cartigny, P., Li, J., 2014. Anomalous nitrogen isotopes in ultrahigh-pressure metamorphic rocks from the Sulu orogenic belt: Effect of abiotic nitrogen reduction during fluid–rock interaction. Earth Planet. Sci. Lett., 403: 67-78.
Li, L., Wing, B.A., Bui, T.H., McDermott, J.M., Slater, G.F., Wei, S., Lacrampe-Couloume, G., Sherwood Lollar, B., 2016. Sulfur mass-independent fractionation in subsurface fracture waters indicates a long-standing sulfur cycle in Precambrian rocks. Nature Communications, 7: 1325. Doi: 10.1038/ncomms13252.
Li, L., Li, K., Li, Y., Zhang, J., Du, Y., Labbe, M., 2021a. Recommendations for combustion-based nitrogen isotope analysis for silicate minerals and rocks. Rapid Comm. Mass Spectrometry, 35: e9075. Doi: 10.1002/rcm.9075.
Li, L., He, Y., Zhang, Z., Liu, Y., 2021b. Nitrogen isotope fractionations among gaseous and aqueous NH_4^+, NH_3, N_2 and metal-ammine complexes: Theoretical calculations and applications. Geochim. Cosmochim. Acta, 295: 80-97.
Li, Y., Li, L., Wu, Z., 2021c. First-principles calculations of equilibrium nitrogen isotope fractionations among aqueous ammonium, silicate minerals and salts. Geochim. Cosmochim. Acta, 297: 220-232.
Li, L., Cartigny, P., Li, K., 2021d. Experimental investigation of formation and decomposition of roaldite in ammonia atmosphere at 300-700° C and associated nitrogen isotope fractionations. Geochim. Cosmochim. Acta, 300: 65-78.
Lightfoot, P.C., Farrow, C.E.G., 2002. Geology, geochemistry, and mineralogy of the Worthington Offset Dike: A genetic model for offset dike mineralization in the Sudbury igneous complex. Econ. Geol., 97: 1419-1446.
Lin, L.-H., Hall, J.A., Lippmann, J., Ward, J., Sherwood Lollar, B., DeFlaun, M., Rothmel, R., Moser, D.P., Gihring, T.M., Mislowack, B., Onstott, T.C., 2005. Radiolytic H_2 in continental crust: Nuclear power for deep subsurface microbial communities. Geochem. Geophys. Geosyst., 6: Q07003.
Lin, L.-H., Wang, P.-L., Lippmann-Pipke, J., Boice, E., Pratt, L.M., Sherwood Lollar, B., Brodie, E.L., Hazen, T.C., Andersen, G.L., DeSantis, T.Z., Moser, D., Kershaw, D.,

Onstott, T.C., 2006. Long-term sustainability of a high-energy, low-diversity crustal biome. Science, 314: 479-482.
Lippmann-Pipke, J., Sherwood Lollar, B., Niedermann, S., Stroncik, N.A., Naumann, R., van Heerden, E., Onstott, T.C., 2011. Neon identifies two billion year old fluid component in Kaapvaal Craton. Chem. Geol., 283: 287-296.
Lippmann, J., Stute, M., Torgersen, T., Moser, D.P., Hall, J.A., Lin, L.-H., Borcsik, M., Bellamy, R.E.S., Onstott, T.C., 2003. Dating ultra-deep mine waters with noble gases and ^{36}Cl, Witwatersrand Basin, South Africa. Geochim. Cosmochim. Acta, 67: 4597-4619.
Lollar, G.S., Warr, O., Telling, J., Osburn, M.R., Sherwood Lollar, B., 2019. 'Follow the Water': Hydrogeochemical constraints on microbial investigations 2.4 km below surface at the Kidd Creek Deep Fluid and Deep Life Observatory. Geomicrobiol. J., 36: 859-872.
Magnabosco, C., Ryan, K., Lau, C.Y.M., Kuloyo, O., Sherwood Lollar, B., Kieft, T., van Heerden, E., onstott, T.C., 2015. A metagenomic window into carbon metabolism at 3 km depth in Precambrian Continental Crust. The ISME Journal, 10: 730-741.
Magnabosco, C., Timmers, P.H.A., Lau, M.C.Y., Borgonie, G., Linage-Alvarez, B., Kuloyo, O., Alleva, R., Kieft, T.L., Slater, G.S., van Heerden, E., Sherwood Lollar, B., Onstott, T.C., 2018. Fluctuations in populations of subsurface methane oxidizers in coordination with changes in electron acceptor availability. FEMS Microb. Ecol., 94: doi: 10.1093/femsec/fiy089.
Meldrum, A., AbdelRahman, A.F.M., Martin, R.F., Wodicka, N., 1997. The nature, age and petrogenesis of the Cartier batholith, northern flank of the Sudbury structure, Ontario, Canada. Precam. Res., 82: 265-285.
Mercier-Langevin, P., Dubé, B., Hannington, M.D., davis, D.W., Lafrance, B., Goseelin, G., 2007. The LaRonde Penna Au-rich volcanogenic massive sulfide deposit, Abitibi greenstone belt, Quebec: Part I. geology and geochronology. Econ. Geol., 102: 585-609.
Montgomery, J., 1994. An isotopic study of CH_4 and associated N_2 and H_2 gases in Canadian Shield mining environments. MSc Thesis. University of Toronto.
NASEM (National Academies of Sciences, Engineering, and Medicine), 2019. An Astrobiology Strategy for the Search for Life in the Universe. The National Academies Press, Washington, D.C. https://doi.org/10.17226/25252.
Onstott, T.C., Lin, L.-H., Davidson, M., Mislowack, B., Borcsik, M., Hall, J., Slater, G.F., Ward, J.A., Sherwood Lollar, B., Lippmann-Pipke, J., Boice, E., Pratt, L.M., Pfiffner, S., Moser, D.P., Gihring, T.M., Kieft, T.L., Phelps, T.J., van Heerden, E., Litthaur, D., DeFlaun, M., Rothmel, R., Wanger, G., Southam, G., 2006. The origin and age of biogeochemical trends in deep fracture water of the Witwatersrand Basin, South Africa. Geomicrobiol. J., 23: 369-414.
Paktunç, A., 1984. Metamorphism of the ultramafic rocks of the Thompson mine, Thompson Nickel Belt, northern Manitoba. Can. Mineral., 22: 77-91.
Powell, W.G., Carmichael, D.G., Hodgson, C.J., 2011. Conditions and timing of metamorphism in the southern Abitibi Greenstone Belt, Quebec. Can. J. Earth Sci., 32: 787-805.
Prior, G.J., Gibson, H.L., Watkinson, D.H., Cook, R.E., 1999. Anatomy, lithogeochemistry, and emplacement mechanisms for the QP rhyolite, Kidd Creek mine, Timmins, Ontario. In: Hannington, M.D., Barrie, C.T. (Eds.), Economic Geology Monograph 10: The Giant Kidd Creek Volcanogenic Massive Sulfide Deposit, Western Abitibi Subprovince, Canada. the Economic Geology Publishing Co., pp. 123-142.

Sadofsky, S. J. and Bebout, G.E., 2004. Nitrogen geochemistry of subducting sediments: New results from the Izu-Bonin-Mariana margin and insights regarding global nitrogen subduction. Geochem. Geophys. Geosyst., 5: Q03I15, doi:10.1029/2003GC000543.

Sherwood Lollar, B., Frape, S.K., Fritz, P., Macko, S.A., Welhan, J.A., Blomqvist, R., Lahermo, P.W., 1993a. Evidence for bacterially generated hydrocarbon gas in Canadian Shield and Fennoscandian Shield rocks. Geochim. Cosmochim. Acta, 57: 5073-5085.

Sherwood Lollar, B., Frape, S.K., Weise, S.M., Fritz, P., Macko, S.A., Welhan, J.A., 1993b. Abiogenic methanogenesis in crystalline rocks. Geochim. Cosmochim. Acta, 57: 5087-5097.

Sherwood Lollar, B., Heuer, V., McDermott, J.M., Tille, S., Warr, O., Moran, J.J., Telling, J., Hinrichs, K.-U., 2021. A window into the abiotic carbon cycle - Acetate and formate in fracture waters in 2.7 billion year-old host rocks of the Canadian Shield. Geochim. Cosmochim. Acta, 294: 295-314.

Sherwood Lollar, B., Westgate, T., Ward, J., Slater, G.F., Lacrampe-Couloume, G., 2002. Abiogenic formation of alkanes in the Earth's crust as a minor source for global hydrocarbon reservoirs. Nature, 416: 522-524.

Sherwood Lollar, B., Lacrampe-Couloume, G., Slater, G.F., Ward, J., Moser, D.P., Gihring, T.M., Lin, L.-H., Onstott, T.C., 2006. Unravelling abiogenic and biogenic sources of methane in the Earth's deep subsurface. Chem. Geol., 226: 328-339.

Sherwood Lollar, B., Lacrampe-Couloume, G., Voglesonger, K., Onstott, T.C., Pratt, L.M., Slater, G.F., 2008. Isotopic signatures of CH_4 and higher hydrocarbon gases from Precambrian Shield sites: a model for abiogenic polymerization of hydrocarbons. Geochim. Cosmochim. Acta, 72: 4778-4795.

Sherwood Lollar, B., Onstott, T.C., Lacrampe-Couloume, G., Ballentine, C.J., 2014. The contribution of the Precambrian continental lithosphere to global H_2 production. Nature, 516: 379-382.

Sherwood Lollar, B., Voglesonger, K., Lin, L.-H., Lacrampe-Couloume, G., Telling, J., Abrajano, T.A., Onstott, T.C., Pratt, L.M., 2007. Hydrogeologic controls on episodic H_2 release from Precambrian fractured rocks - Energy for deep subsurface life on Earth and Mars. Astrobiology, 7: 971-986.

Sheik, C.S., Badalamenti, J.P., Telling, J., Hsu, D., Alexander, S.C., Bond, D.R., Gralnick, J.A., Sherwood Lollar, B., Toner, B.M., 2021. Novel microbial groups drive productivity in an Archean iron formation. Front. Microbiol., 12: doi: 10.3389/fmicb.2021.627595.

Silver, B.J., Raymond, R., Sigman, D.M., Prokopeko, M., Sherwood Lollar, B., Lacrape-Coulome, Fogel, M.L., Pratt, L.M., Lefticariu, L., Onstott, T.C., 2012. The origin of NO_3^- and N_2 in deep subsurface fracture water of South Africa. Chem. Geol., 294-295: 51-62.

Slack, P.B., 1974. Variance of terrestrial heat flow between the North American Craton and the Canadian Shield. Geol. Soc. Amer. Bullet., 85: 519-522.

Smirnov, A., Hausner, D., Laffers, R., Strongin, D.R., Schoonen, M., 2008. Abiotic ammonium formation in the presence of Ni-Fe metals and alloys and its implications for the Hadean nitrogen cycle. Geochem. Trans., 9: 5. Doi: 10.1186/1467-4866-9-5.

Smith, P.E., Schandl, E.S., York, D., 1993. Timing of metasomatic alteration of the Archean Kidd Creek massive sulfide deposit, Ontario, using ^{40}Ar- ^{39}Ar laser dating of single crystals of fuchsite. Econ. Geol., 88: 1636-1642.

Telling, J., Voglesonger, K., Sutcliffe, C.N., Lacrampe-Couloume, G., Edwards, E., Sherwood Lollar, B., 2018. Bioenergetic constraints on microbial hydrogen utilization in Precambrian deep crustal fracture fluids. Geomicrobiol. J., 35: 108-119.

Thompson, L.M., Spray, J.G., Kelley, S.P., 1998. Laser probe argon-40/argon-39 dating of pseudotachylyte from the Sudbury Structure: Evidence for postimpact thermal overprinting in the North Range. Meteor. Planet. Sci., 33: 1259-1269.

Ward, J., Slater, G., Moser, D., Lin, L.-H., Lacrampe-Couloume, G., Bonin, A.S., Davidson, M., Hall, J.A., Mislowack, B., Bellamy, R.E.S., Onstott, T.C., Sherwood Lollar, B., 2004. Microbial hydrocarbon gases in the Witwatersrand Basin, South Africa: Implications for the deep biosphere. Geochim. Cosmochim. Acta, 68: 3239-3250.

Warr, O., Sherwood Lollar, B., Fellowes, J., Sutcliffe, C.N., McDermott, J.M., Holland, G., Mabry, J.C., Ballentine, C.J., 2018. Tracing ancient hydrogeological fracture network age and compartmentalisation using noble gases. Geochim. Cosmochim. Acta, 222: 340-362.

Warr, O., Giunta, T., Ballentine, C.J., Sherwood Lollar, B., 2019. Mechanisms and rates of ^{4}He, ^{40}Ar, and H_2 production and accumulation in fracture fluids in Precambrian Shield environments. Chem. Geol., 530: 119322.

Warr, O., Giunta, T., Onstott, T.C., Kieft, T., Harris, R.L., Nisson, D.M., Sherwood Lollar, B., 2021a. The role of low-temperature ^{18}O exchange in the isotopic evolution of deep subsurface fluids. Chem. Geol., 561: 120027.

Warr, O., Young, E.D., Giunta, T., Kohl, I., Ash, J., Sherwood Lollar, B., 2021b. High-resolution, long-term isotopic and isotopologue variation identifies the sources and sinks of methane in a deep subsurface carbon cycle. Geochim. Cosmochim. Acta, 294: 315-334.

Wilpiszeski, R.L., Sherwood Lollar, B., Warr, O., House, C.H. (2020) In situ growth of halophilic bacteria in saline fracture fluids from 2.4 km below surface in the deep Canadian Shield. Life, 10: 307. Doi: 10.3390/life10120307.

Yeung, L.Y., Li, S., Kohl, I.E., Haslun, J.A., Ostrom, N.E., Hu, H., Fischer, T.P., Schauble, E.A., Young, E.D., 2017. Extreme enrichment in atmospheric 15N15N. Science Advances, 3: Article eaao6741.

Young, E.D., Kohl, I.E., Sherwood Lollar, B., Etiope, G., Rumble, D., Li, S., Haghnegahdar, M. A., Schauble, E.A., McCain, K.A., Foustoukos, D.I., Sutcliffe, N.C., Warr, O., Ballentine, C.J., Onstott, T.C., Hosgormez, H., Neubeck, A., Marques, J.M., Perez-Rodriguez, I., Rowe, A.R., LaRowe, D.E., Magnabosco, C., Bryndzia, T., 2017. The relative abundances of resolved $^{12}CH_2D_2$ and $^{13}CH_3D$ and mechanisms controlling isotopic bond ordering in abiotic and biotic methane gases. Geochim. Cosmochim. Acta, 203: 235-264.

Zwanzig, H.V., Macek, J.J., McGregor, C.R., 2007. Lithostratigraphy and geochemistry of the high-grade metasedimentary rocks in the Thompson nickel belt and adjacent Kisseynew domain, Manitoba: implications for nickel exploration. Econ. Geol., 102: 1197-1216.

Figure captions

Fig. 1. Location map of sample sites for this study together with the sites with $\delta^{15}N_{N2}$ values reported in Sherwood Lollar et al. (1993a). The general geology of the Canadian Shield is shown in the inserted panel (revised from Hoffmann, 1989; Li et al., 2016; Warr et al., 2019). BT = Birchtree; TH = Thompson; KC = Kidd Creek; FR = Fraser; NR = Nickel Rim; CCS = Copper Cliff South; LR = LaRonde; VDO = Val D'Or; NT = Norita

Fig. 2. Comparison of $\delta^{15}N$ values of N_2 with N_2/O_2 ratio (A) and N_2/Ar ratio (B, C) for subsurface fracture waters from the Canadian Shield. Error bars are smaller than data symbols. These highly reducing fracture waters produce H_2 and do not contain O_2, thus the N_2/O_2 ratio can be used as a robust index for air contamination. The vertical line (N_2/O_2 = 15) in panel A divides significantly contaminated samples to the left and less contaminated samples to the right. In contrast, the fracture waters contain various amounts of ^{40}Ar (and N_2/Ar ratio) from the decay of ^{40}K in host rocks. Thus N_2/Ar ratios cannot be used to quantify the air component. All samples with known N_2/Ar ratios $\delta^{15}N$ values are compiled in Panel B. Whereas only samples with known N_2/O_2 values of >15 are plotted in panel C. Historical samples marked by "(M)" are unpublished thesis data from Montgomery (1994); samples marked by "(BSL)" are from Sherwood Lollar et al. (1993a). Both are shown as filled grey symbols.

Fig. 3. Comparison of $\delta^{15}N$ values of N_2 in subsurface fracture waters from the Kaapvaal Craton (A), the Fennoscandian Shield (B), and the Canadian Shield (C). The Canadian Shield samples are consistently more ^{15}N enriched than those from the other two cratons. See text for discussion.

Fig. 4. Comparison of $\Delta^{15}N_{N2\text{-}rock}$ between observed values and theoretical values of metamorphic devolatilization calculated by Rayleigh fractionation modeling (A-C), and increase in $\delta^{15}N$ of N_2 (expressed as $\Delta^{15}N_{Remianing\ N2\text{-}initial\ N2}$) after abiotic nitrogen reduction (D-F). The f in both panels denote the fraction of remaining nitrogen in the reactant. See text for discussion.

Fig. 5. Diagram showing steady decrease in the $\delta^{15}N$ value of N_2 from one single borehole at 2.4 km below surface of the Kidd Creek mine over a 10-year period.

Figure 1

Click here to access/download;Figure;Fig.

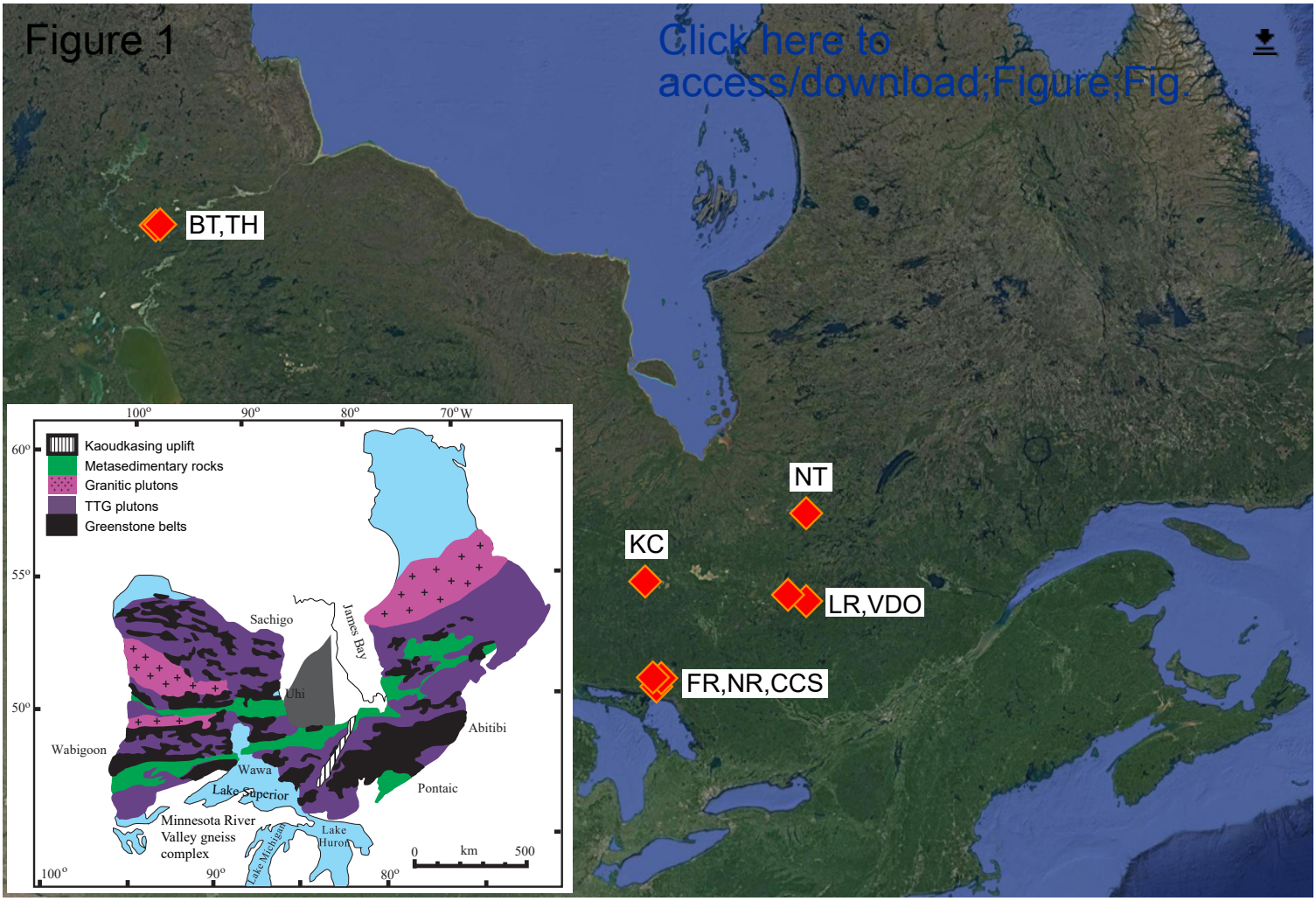

Figure 2

Click here to access/download;Figure;Fig. 2.pdf

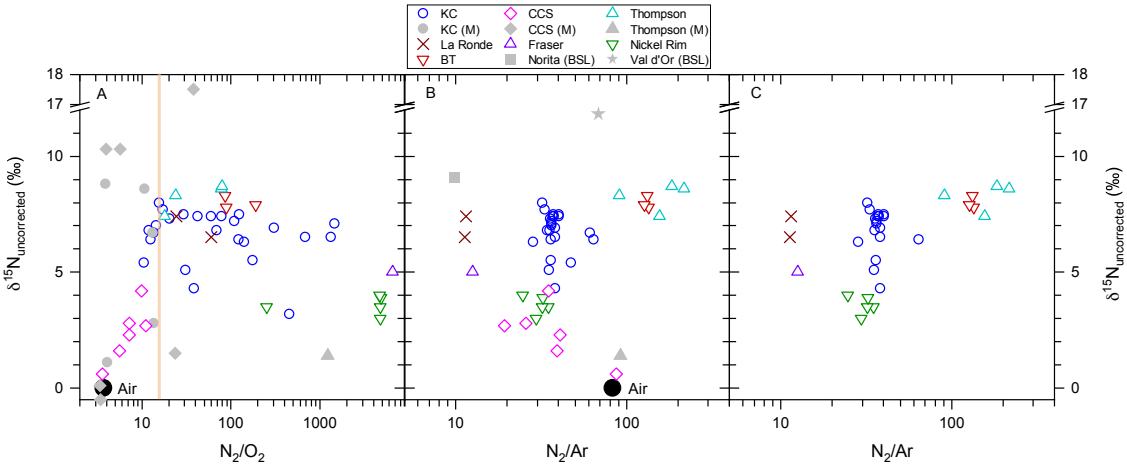

Figure 3

Click here to access/download;Figure;Fig. 3.pdf

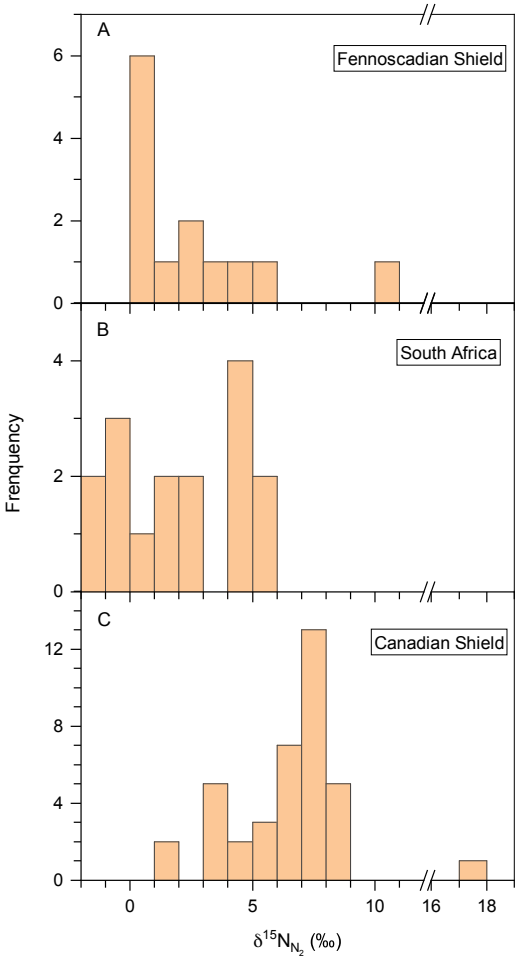

Figure 4

Click here to access/download;Figure;Fig. 4.pdf

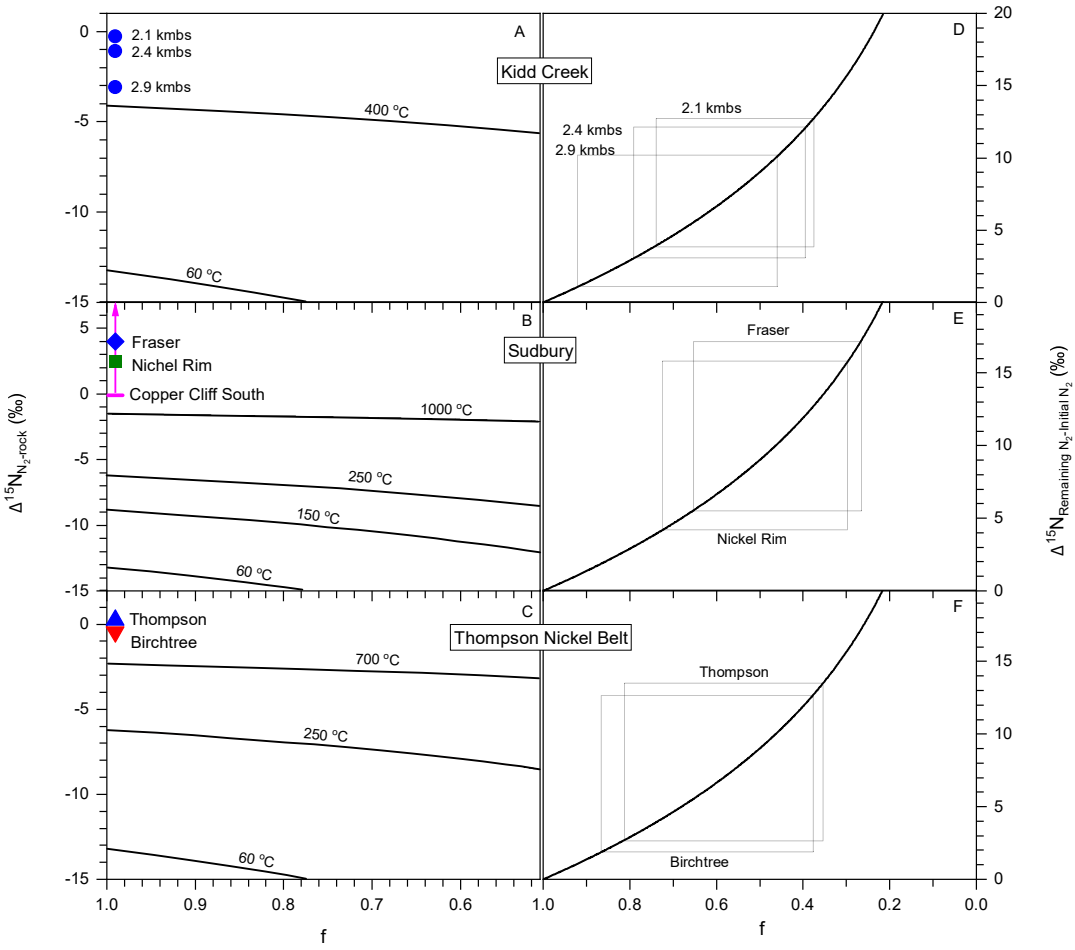

Figure 5

Click here to access/download;Figure;Fig. 5.pdf

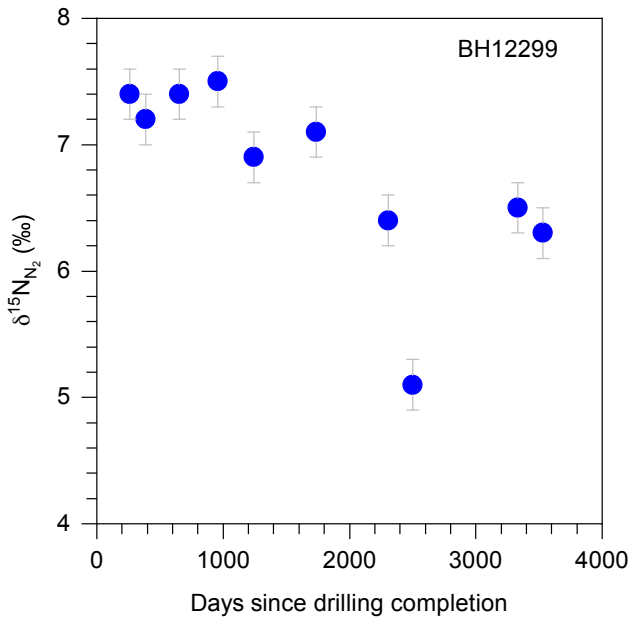

Table1. Major components§ and $\delta^{15}N_{N2}$ value of gas samples from deep subsurface fracture fluids in the Canadian Shield.

Location	Sample ID	H_2 (vol%)	He (vol%)	Ar (vol%)	O_2 (vol%)	CH_4 (vol%)	N_2 (vol%)	N_2/O_2	N_2/Ar	$\delta^{15}N_{N2}$ (‰)
Kidd Creek	10.1.2000-KCL6900-1F	0.33	n.d.	0.23	0.66	75.05	7.93	12.0	34.5	6.8
	10-1-2000-KCL6900-2D	1.95	n.d.	0.29	0.60	73.60	9.32	15.5	32.1	8.0
	10-1-2000-KCL6900-3A	2.47	n.d.	0.34	0.66	72.48	11.31	17.1	33.3	7.7
	10-1-2000-KCL6900-4D	1.32	n.d.	0.35	0.88	70.48	12.69	14.4	36.3	7.0
	10-1-2000-KCL6900-5D	2.03	n.d.	0.39	0.69	70.70	14.01	20.3	35.9	7.3
	10-1-2000-KCL6900-6B	1.40	n.d.	0.33	0.95	75.08	11.90	12.5	36.1	6.4
	12.2.2008-KC7850-12261	3.16	2.45	0.39	0.20	72.15	13.84	69.2	35.5	6.8
	10.5.2007-KC7850-12262	8.37	2.91	0.35	0.48	69.10	14.03	29.2	40.1	7.5
	22.10.2015-KC7850-12262	2.7	2.00	0.43	1.96	56.70	26.40	13.5	61.4	6.7
	27.8.2007-KC7850-12287A	10.67	2.47	0.34	1.54	72.17	16.10	10.5	47.4	5.4
	20.6.2008-KC7850-12287A	3.61	2.45	0.36	0.24	70.10	14.45	60.2	40.1	7.4
	12.2.2008-KC7850-12299	6.52	2.15	0.45	0.40	71.98	16.87	42.2	37.5	7.4
	19.6.2008-KC7850-12299	3.32	2.42	0.42	0.14	67.70	15.35	109.6	36.5	7.2
	31.3.2009-KC7850-12299	4.82	2.87	0.40	0.19	64.37	14.81	77.9	37.0	7.4
	12.01.2010-KC7850-12299	4.62	2.54	0.40	0.12	71.49	14.94	124.5	37.4	7.5
	21.10.2010-KC7850-12299	3.97	2.62	n.d.	<0.05	70.32	15.32	> 306.4		6.9
	29.2.2012-KC7850-12299	3.19	2.39	n.d.	<0.01	71.92	14.60	> 1460.0		7.1
	20.09.2013-KC7850-12299	5.58	2.69	0.21	0.11	70.98	13.50	122.7	64.3	6.4
	02.04.2014-KC7850-12299	2.52	1.60	0.28	0.32	74.6	9.88	30.9	35.3	5.1
	12.07.2016-KC7850-12299*	3.60	2.41	0.35	<0.01	71.3	13.36	> 1336.0	38.2	6.5
	25.01.2017-KC7850-12299*	4.80	3.70	0.54	0.11	71.6	15.40	140.0	28.5	6.3
	08.2.2012-KC9500-13675	<0.01	1.63	n.d.	<0.01	78.70	4.53	> 453.0		3.2
	1.3.2012-KC9500-13684	5.30	2.10	n.d.	<0.01	75.83	6.80	> 680.0		6.5
	29.11.2012-KC9500-BH2	16.6	0.43	0.29	0.06	71.0	10.50	175.0	36.2	5.5
	13.07.2016-KC9500-bubA	0.70	1.77	0.27	0.27	71.6	10.34	38.3	38.3	4.3
LaRonde	24.03.2016-LR6480-L2900-LR-290-	1.83	5.09	1.33	0.63	66.11	15.25	24.2	11.5	7.4
	24.03.2016-LR6480-L2900-LR-290-	3.63	7.20	0.79	0.15	72.10	8.92	59.5	11.3	6.5

Location	Sample ID	H_2 (vol%)	He (vol%)	Ar (vol%)	O_2 (vol%)	CH_4 (vol%)	N_2 (vol%)	N_2/O_2	N_2/Ar	$\delta^{15}N_{N2}$ (‰)
Copper Cliff South	CCSM-GH-11-7-2001-1E	54.00	3.46	0.07	0.40	33.15	2.87	7.2	41.0	2.3
	CCSM-GH-11-7-2001-2E	43.00	3.38	0.23	5.54	14.68	20.02	3.6	87.0	0.6
	CCSM-GH-11-7-2001-3D	9.94	4.37	0.16	0.57	70.19	5.61	9.8	35.1	4.2
	CCSM-GH-11-7-2001-5E	57.59	2.62	0.07	0.49	23.96	2.74	5.6	39.1	1.6
	CCSM-GH-11-7-2001-6E	51.00	6.42	0.12	0.43	31.79	3.10	7.2	25.8	2.8
	CCSM-GH-11-7-2001-7E	19.7	2.52	0.28	0.49	57.97	5.41	11.0	19.3	2.7
Nickel Rim	29.11.2013-NR1730m_NR170128	0.01	32.23	1.51	0.21	15.40	52.65	250.7	34.9	3.5
	05.03.2014-NR1730m_NR170128	0.03	29.90	1.50	<0.01	19.38	48.09	> 4809.0	32.1	3.5
	05.03.2014-NR1730m_NR170182	1.64	27.73	1.51	<0.01	n.a.	48.87	> 4887.0	32.4	3.9
	05.03.2014-NR1730m_NR170183	2.67	26.19	1.91	<0.01	24.29	47.35	> 4735.0	24.8	4.0
	22.10.2014-NR1730m_NR170128	0.01	24.12	1.61	<0.01	24.34	47.73	> 4773.0	29.6	3.0
Fraser	06.03.2014_FML4700_FR47774	<0.01	16.68	5.24	<0.01	19.82	65.76	> 6576.0	12.5	5.0
Birchtree	28.5.2007-BT3950L-gas stopper BH	0.02	1.35	0.22	0.34	62.9	29.26	86.1	133.0	8.3
	6-11-2007-BT3900-9167N-BH (Floor#2)	<0.005	1.38	0.23	0.35	68.7	30.92	88.3	134.4	7.8
	27-3-2008-BT3900-9167N-BT1	0.08	1.33	0.24	0.16	62.9	30.54	190.9	127.3	7.9
Thompson	1065750 13.06.06 (3-403-2)	2.75	2.40	0.51	1.92	34.7	46.26	24.1	90.7	8.3
	1065760 14.06.06 (1-401-2)	0.79	2.70	0.42	3.63	36.5	65.51	18.0	156.0	7.4
	1163630 13.06.06 (7-399-5)	0.30	2.99	0.28	0.77	36.6	60.77	78.9	217.0	8.6
	1065800 13.06.06 (4-405-3)	0.03	2.80	0.28	0.65	45.5	51.78	79.7	184.9	8.7

[§] Major Gas contents of these samples have been reported by Sherwood Lollar et al., 2006; Li et al. (2016); Telling et al. (2018); Warr et al. (2019). The contents of N_2, Ar, and O_2 reported here, if slightly different to those in the literature, were re-analyzed results on the same gas bottle used for $\delta^{15}N_{N2}$ analysis.

[*] Labidi et al. (2020) reported $\delta^{15}N$ values of 6.6‰ for sample 12.07.2016-KC7850-12299 and 6.7‰ for sample 25.01.2017-KC7850-12299.

Table 2. $\delta^{15}N$ values of rock samples from Kidd Creek, Sudbury, and Thompson

Location	Sample ID	Lithology	Bulk-rock N (ppm)	Bulk-rock $\delta^{15}N$ (‰)	Reduced carbon component $\delta^{15}N$ (‰)
Kidd Creek	BH12612A (465.30-465.62 m)	Graphite-bearing lens	68.9	7.0	7.0
	BH12612A (470.50-470.96 m)	Graphite-bearing lens	67.6	6.7	6.7
	BH12612A (392.80-393.15 m)	Graphite-bearing lens	98.6	9.3	
	BH12612A (413.38-413.75 m)	Graphite-bearing lens	40.5	8.7	1.3
	BH12299 (369.5 m)	Graphite-bearing lens	54.9	15.6	10.4
	BH12299 (472.4 m)	Graphite-bearing lens	89.8	10.2	0.4
		Average	**70.1**	**9.6**	**5.2**
	BH12612A (232.10-232.26 m)	Rhyolite	30.9	7.8	
	BH12612A (243.30-243.07 m)	Rhyolite	22.7	7.3	
	BH12612A (248.80-249.35 m)	Rhyolite	34.3	6.0	
	BH12612A (292.70-293.15 m)	Silicified cherty breccia	23.0	10.3	
	BH12612A (353.20-353.38 m)	Silicified cherty breccia	11.9	10.4	
	BH12612A (475.85-476.02 m)	Quartz feldspar porphyry	19.3	6.3	
		Average	**23.7**	**8.0**	
Sudbury	Creighton Mine BH131106 (395.50-396.60 m)	Meta-gabbro	14.1	2.6	
	Creighton Mine BH131106 (395.50-396.60 m)	Breccia matrix	14.9	2.3	
		Average	**14.5**	**2.4**	
	Nickel Rim BH130075 (319.96-320.14m)	Felsic gneiss	12.7	1.3	
	Nickel Rim BH170143 (75.87-76.07m)	Felsic norite	13.6	3.4	
	Nickel Rim BH170143 (109.98-110.16 m)	Felsic norite	49.3	-5.6	
	Nickel Rim BH170143 (178.00-178.20 m)	Granodiorite	9.7	2.2	
	Nickel Rim BH170143 (283.91-284.04 m)	Felsic gneiss	12.3	3.1	
	Nickel Rim BH170143 (349.90-364.11)	Breccia	10.0	1.8	
		Average	**17.9**	**1.0**	
Thompson	Thompson mine assorted core	Archean gneiss	30.2	7.0	
	Thompson mine assorted core	Thompson Formation skarn	50.9	8.1	
	Thompson mine assorted core	schist	50.2	10.2	
		Average	**43.8**	**8.4**	